

# Social learning across symbolic cultural barriers in non-human cultures

Antonio Leitao,<sup>1,2</sup> Maxime Lucas,<sup>1,2</sup> Simone Poetto,<sup>1,2,3</sup> Taylor A. Hersh,<sup>4</sup> Shane Gero,<sup>2,5,6</sup> David Gruber,<sup>2,7</sup> Michael Bronstein,<sup>2,8</sup> and Giovanni Petri<sup>1,2,9,10</sup>

<sup>1</sup>*CENTAI Institute, Corso Inghilterra 3, 10138 TO, Italy*

<sup>2</sup>*Project CETI, New York, NY, 10003 USA*

<sup>3</sup>*Center for Modern Interdisciplinary Technologies, Nicolaus Copernicus University, Toruń, Poland*

<sup>4</sup>*Comparative Bioacoustics Group, Max Planck Institute for Psycholinguistics, Nijmegen, Netherlands*

<sup>5</sup>*Department of Biology, Carleton University, Ottawa, Ontario, Canada*

<sup>6</sup>*The Dominica Sperm Whale Project, Roseau, Dominica*

<sup>7</sup>*Department of Natural Sciences, City University of New York, Baruch College, New York, NY, United States,*

<sup>8</sup>*Department of Computer Science, University of Oxford, Oxford, UK*

<sup>9</sup>*NPLab, Network Science Institute, Northeastern University London, London, UK*

<sup>10</sup>*IMT Lucca, Lucca, Italy*

(Dated: July 12, 2023)

Social learning is key in the development of both human and non-human animal societies. Here, we provide quantitative evidence that supports the existence of social learning in sperm whales across socio-cultural barriers, based on acoustic data from locations in the Pacific and Atlantic Oceans. Sperm whale populations have traditionally been partitioned into clans based on their *vocal repertoire* (what they say) of rhythmically patterned clicks (codas), and in particular their *identity codas*, which serve as symbolic markers for each clan. However, identity codas account for between 35% and 60% of all codas vocalized depending on the different clans. We introduce a computational modeling approach that recovers clan structure and shows new evidence of social learning across clans from the internal temporal structure of *non-identity codas*, the remaining fraction of codas. The proposed method is based on *vocal style*, which encodes *how* sperm whales assemble individual clicks into codas. Specifically, we modeled clicking pattern data using generative models based on variable length Markov chains, producing what we term “subcoda trees”. Based on our results, we propose here a new concept of *vocal identity*, which consists of both vocal repertoire and style. We show that (i) style-delimited clans are similar to repertoire-delimited clans, and that (ii) sympatry increases vocal style similarity between clans for non-identity codas, but has no significant effect on identity codas. This implies that different clans who geographically overlap have similar styles for most codas, which in turn implies social learning across cultural boundaries. More broadly, the proposed method provides a new framework for comparing communication systems of other animal species, with potential implications for our understanding of cultural transmission in animal societies.

## I. INTRODUCTION

Cultural transmission is defined as the transmission of information or behaviors between individuals of the same species by means of social learning [1]. While humans represent the pinnacle of such capacity, cultural transmission has been observed in a wide variety of animals, including cetaceans [2, 3], songbirds [4], non-human primates [5], and insects [6].

When animals have the capacity for social learning, group-specific differences can arise and remain stable when they become distinguishable by symbolic markers: arbitrary group-identity signals that are recognizable by both members of the group itself and by members of other groups [7, 8]. In humans, symbolic markers can take a myriad of forms, ranging from visible signs, such as tattoos or garments, to communication cues or signals, such as idiomatic sentences or accents [7–9]. In animals, however, quantitative evidence of symbolic markers is remarkably scarce, one exception being recent results on the use of *identity codas* in sperm whale social communication [10].

Sperm whales live in multi-tiered societies and have a

complex vocal communication system [11]. They communicate through rhythmic patterns (*codas*) of short broadband sounds (*clicks*), which have traditionally been classified into a finite set of *coda types* based on the total number of clicks, their rhythm, and their tempo [12, 13].

The combination of the set of used coda types (*coda usage*) and how frequently each is used (*coda frequency*) makes up a *vocal repertoire*. While there is evidence of individual variation in vocal repertoires [14–16], sperm whales belonging to the same social unit—a stable, matrilineally-based group of whales—share a similar vocal repertoire which is stable across years [15–17]. Social units that share substantial parts of their repertoire are said to be part of the same *vocal clan* [18, 19]. There is clear social segregation between members of different clans, even when living in sympatry, and thus clans mark a higher level of social organization, which appears to be defined on the basis of cultural vocal markers [10, 18, 19].

The clan specificity and redundant usage of certain coda types, termed *identity codas* [10, 13], align with the expectations for symbolic markers of group membership [8]. Furthermore, quantitative evidence that sperm whales themselves use identity codas as such markers has

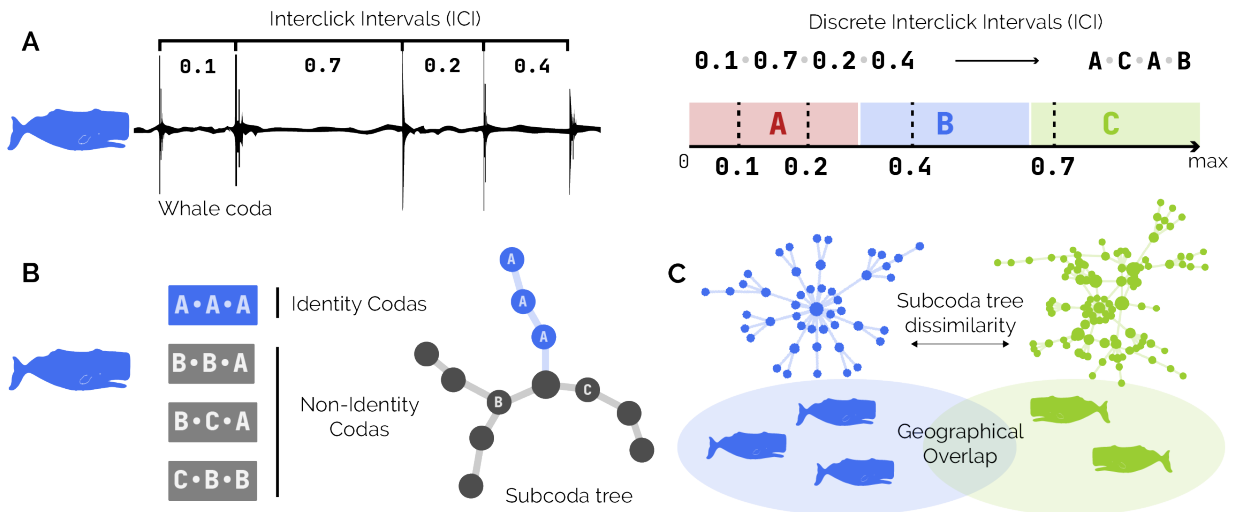


**FIG. 1. Statistical modeling of sperm whale communication: our analytical pipeline.** Sperm whale communication consists of rhythmic sequences of clicks, called codas. **A** First, we represented codas as sequences of discrete Inter-Click intervals (dICIs), by fitting absolute ICIs into bins (A, B, C, ...). Here, the waveform of a five-click coda is shown. **B** Then, we modeled these sequences with variable-length Markov chains, which can be visualized as *subcode trees*. These trees can be built for an individual speaker or a group of speakers, and capture the internal structure of codas and hence of sperm whale communication. Whale social units are divided into clans according to their coda usage and repertoire. Each clan has coda types that are used to identify their clan, called ID codas [10]. Only about 35% of all emitted codas are ID codas. All other codas are non-ID. **C** The distance between trees can be calculated to compare the similarity of the communication between (groups of) speakers, and compared with other factors, such as geographical clan overlap (see Methods).

recently emerged: the more two clans overlap in geographic space, the more different their identity coda usage repertoires are [10]. This is consistent with computational models [8] of the evolution of symbolic marking, which predict that differences between cultural norms will be starkest when inter-group interactions are more common (e.g., in boundary or overlap regions).

All remaining coda types have been referred to as *non-identity* (non-ID) *codas* and constitute a very large fraction of sperm whales’ total number of coda utterances. In fact, the total number of emitted non-ID codas accounts for more than 6 out of 10 codas (see SM Section 1.1 for the counts per clan and per coda type). This begets the question: if ID codas are used as clan identity signals, what can be said about the remaining 65% of codas?

Here we develop a novel descriptive framework that focuses on the temporal *subcode structure*, the variations of intervals between successive clicks within codas. We find that these modulations within codas characterize an individual’s social unit and clan, effectively fingerprinting coda repertoires from the same clan with something comparable to a clan “accent.” We call the way in which individual codas are assembled *vocal style*, as opposed to the *vocal repertoire*.

Thus, we propose a new concept for *vocal identity* of sperm whales that comprises both style and repertoire.

Crucially, we find that the vocal style of non-ID codas is more similar for more sympatric (i.e., spatially overlapping) clans. In contrast, we do not find an effect of sympatry on the similarity of vocal styles when studying

only ID codas. This suggests that geographic overlap induces vocal styles to become more similar between clans, without jeopardizing each clan’s acoustic identity signals. Our results strengthen previous results on the use of ID codas as symbolic markers, while providing strong evidence of cultural transmission and social learning of vocalizations among whales of *different* clans, as predicted by theoretical models [20].

## RESULTS

### Subcode structure captures variability in sperm whale communication

We model the internal structure of codas at the level of clicks by using variable length Markov chains (VLMCs). Our analytical pipeline is illustrated in Fig. 1. We build each VLMC in two main steps. We first convert codas, naturally represented as sequences of continuous, absolute, inter-click intervals (ICIs), to sequences of discrete ICIs (dICIs), by discretizing time into bins (Fig. 1A). In this way, each dICI represents a narrow range of possible ICI values. The bins have a fixed width  $\delta t$  and thus implicitly correspond to the temporal resolution of our representation (see Methods for details on the optimal choice of  $\delta t$ ). Note that although ICIs have units of time (seconds), dICIs are (unit-less) integers, representing multiples of  $\delta t$ . Hence, each coda (a sequence of ICIs) is mapped to a string of integers (a sequence of dI-

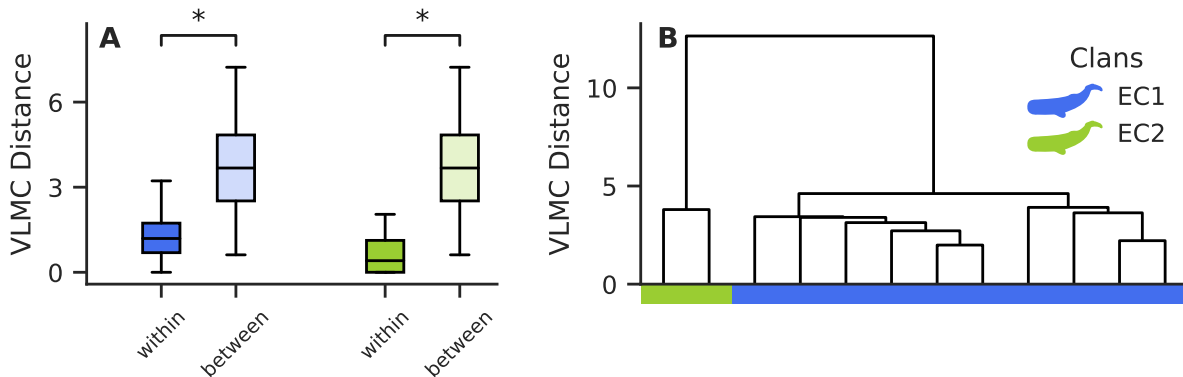


FIG. 2. **Vocal style recovers social structure of vocal clans in Dominica sperm whales.** **A** We show the similarity of vocal style, measured as subcodas tree-distance, among social units within a vocal clan (*within*) and between two clans (*between*). We used the manual clan assignments from [19] as ground truth. Vocal style is more similar within clans than between clans. **B** We show the hierarchical clustering of social unit subcodas trees. Each leaf corresponds to a social unit, and the colors below show their known clan assignments. The clustering recovers the two-clan structure observed in past work [19].

CIIs). The second part of the pipeline focuses on modeling how dICI sequences are assembled from shorter to longer sequences, up to full codas. Essentially, we want to estimate transition probabilities from a dICI sub-sequence to the next dICI (Fig. 1B). A standard way would be to describe this using  $k$ -order Markov chain models, which encode information on previous sub-sequences up to  $k$  steps in the past of the sequence. However, it is possible that different sequences of dICIs contain different amounts of information or memory regarding potential next dICIs. This is akin to what happens with words (e.g., a word beginning with "re" can continue in more ways than one starting with "zy"). To account for this possibility while also retaining only the most compressed statistical representation of how dICIs are assembled in codas, we employ VLMCs.

VLMCs are generalizations of standard (fixed-memory) Markov chains that allow sub-sequences of dICIs of variable lengths, and keep longer sequences only when they are significantly more informative with respect to the previous sequence than random (see Methods for details on model fitting and selection). Furthermore, VLMCs naturally have a tree structure (see Fig. 1B), because they describe the structure of dependencies in transitions from shorter to longer sequences. In particular, each node represents a sub-sequence of dICIs, and is equipped with a probability distribution of transitions to the next dICIs. The origin node corresponds to the empty sequence, leaf nodes correspond to the longest sequences, and all nodes forming the branch in between correspond to the sub-sequences of that leaf node. Thus, we call VLMCs fitted to coda ICI data *subcodas trees*, and represent coda assembly as a walk from the origin node to the leaf nodes. Three more features of subcodas trees are noteworthy: (i) because the method's input is a set of codas, we can build subcodas trees for repertoires corresponding to different social scales, from individual

sperm whales, to social units, all the way up to vocal clans; (ii) the difference between different subcodas trees can be measured using a probabilistic distance (see Methods), which we can use to compare subcodas trees across sperm whale clans; and (iii) subcodas trees can also be used as generative models, to create new synthetic codas in the form of dICI sequences to train downstream machine learning models.

### Vocal style recovers vocal clan structure

The information about vocal style contained in subcodas trees is sufficient to recover the social structure of sperm whales (social units and clans). We show this in two ways. First, we analyze a dataset from sperm whales in Dominica (Dominica dataset) [19]. This dataset has rich annotations (coda type annotations, identity of recorded whales, social relations of recorded whales) which makes it particularly useful for validation. Specifically, sperm whales in the Dominica dataset are divided into two vocal clans, each composed of several social units. For each social unit present in this dataset, we aggregate the individual whales' repertoires and build a subcodas tree. Computing the distance between these trees (see Methods), we find that the distances between social units are significantly smaller within clans than between clans (Fig. 2A). We also find that an agglomerative clustering (average linkage, see Methods for details) on the distance between the subcodas trees correctly clusters social units into their respective clans (Fig. 2B). Without a priori knowledge of the clan memberships, we used vocal style to recover the existing classification of social units into two clans, which was previously done based on similarity between vocal repertoires (i.e., coda types and usage) [19].

Second, we find that the subcodas structure of synthetic

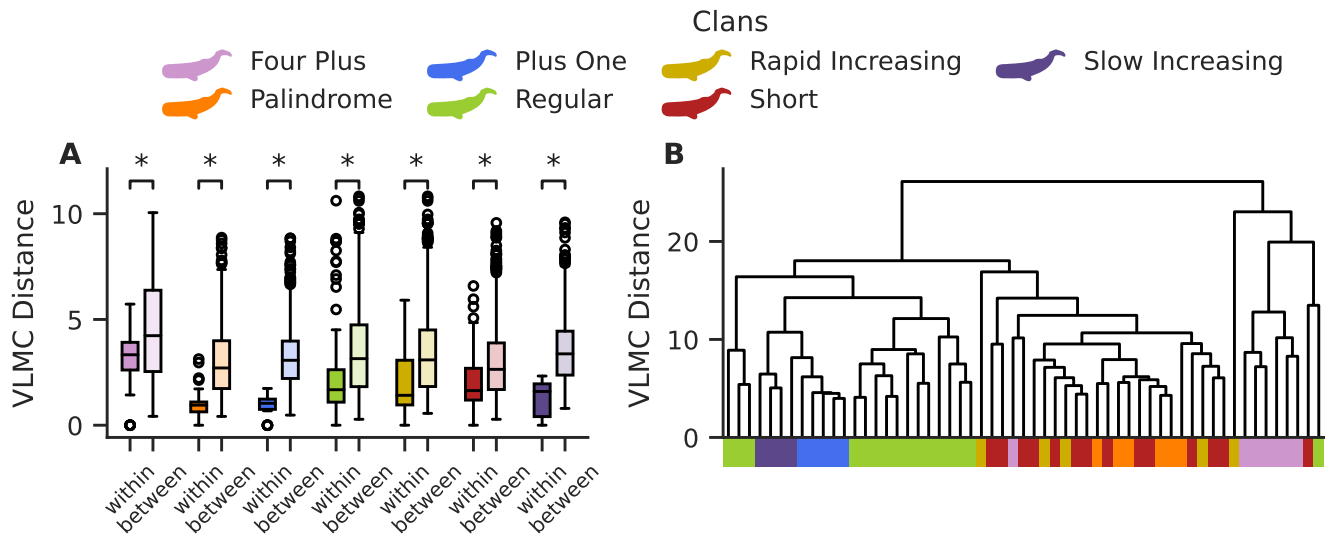


FIG. 3. **Vocal style recovers social structure of vocal clans in Pacific Ocean sperm whales.** **A** We show the similarity of vocal style, measured as subcodas tree-distance, between repertoires within a vocal clan (*within*) and between a clan and all others (*between*). We used the vocal clans identified in [10]. Vocal style is more similar within a clan than between clans. **B** We show the hierarchical clustering of subcodas trees. Each leaf corresponds to a repertoire, and the colors below show their vocal clan assignments (based on vocal repertoires) from [10]. We find generally good overlap between the groups obtained from clustering vocal style and those from vocal repertoire, with the exception of the *Short* clan (red) that is somewhat mixed with the *Palindrome* (orange) and *Rapid Increasing* (yellow) clans.

codas, generated from subcodas trees fitted on real data, closely reproduces that of real codas. To do this, we first train a simple classifier to assign codas to one of the two vocal clans, based on coda type. Variations of the same classifier, trained on the same real data, have been shown to discriminate between individual whales, social units, and clans with high accuracy [21]. We train the classifier on real codas, and then test it on both real and synthetic ones. The synthetic codas were generated using the subcodas tree of each clan, and we made sure the number of codas was similar to that of the original dataset (see Methods for details). We find that synthetic codas are correctly classified into their clans with an accuracy close ( $\sim 85\%$ ) to that obtained on the real data ( $\sim 90\%$ , see *Supplementary Materials* Section 4).

Motivated by these results, we extend our analysis to a much larger dataset from the Pacific Ocean (Pacific dataset) [10]. This dataset is more sparsely annotated because of the breadth of its spatial coverage. We restricted our analyses to a well-sampled subset ( $n = 57$  repertoires) of the full Pacific dataset (see Methods for details). Coda repertoires are only labeled by the spatial position at which they were recorded, but no information is available about the identity of the vocalizing sperm whales (see Methods for details). In fact, each repertoire likely contains codas from multiple individuals of a single clan. It has recently been shown that these repertoires can be divided into seven vocal clans based on their coda usage [10]. We use those clans as a benchmark for the following analysis.

Since there is no social unit-level information for this dataset, we fit a subcodas tree for each repertoire (i.e., all of the codas recorded on a single day in a single region). Trees are significantly more similar for repertoires belonging to the same vocal clan than for those belonging to different vocal clans (Fig. 3A). We also find that clustering repertoires based on vocal style returns a dendrogram that closely matches the one obtained from coda usage in [10] (Fig. 3B). The major exception we find is the *Short* clan (red), named because member whales produce short codas with very few clicks, for which anomalous results were previously reported as well [10]. In our case, this is due to the Short clan being less well localized in the space of trees, while the other clans have well-defined centroids (see *Supplementary Materials* Fig. 9 for a low-dimensional representation subcodas tree metric space).

Therefore, we find that sperm whale vocal clans in the Atlantic Ocean (Caribbean Sea) and Pacific Ocean can be identified by a *vocal identity* that encompasses both clan-specific *repertoire* [10, 18, 19, 22] and *vocal style* as defined in this work.

#### Clan sympatry impacts vocal style of non-ID codas only

While interesting, the fact that both vocal repertoires and vocal styles discriminate between clans might imply that considering both could be redundant for vocal identity. However, we find that this is not the case when we

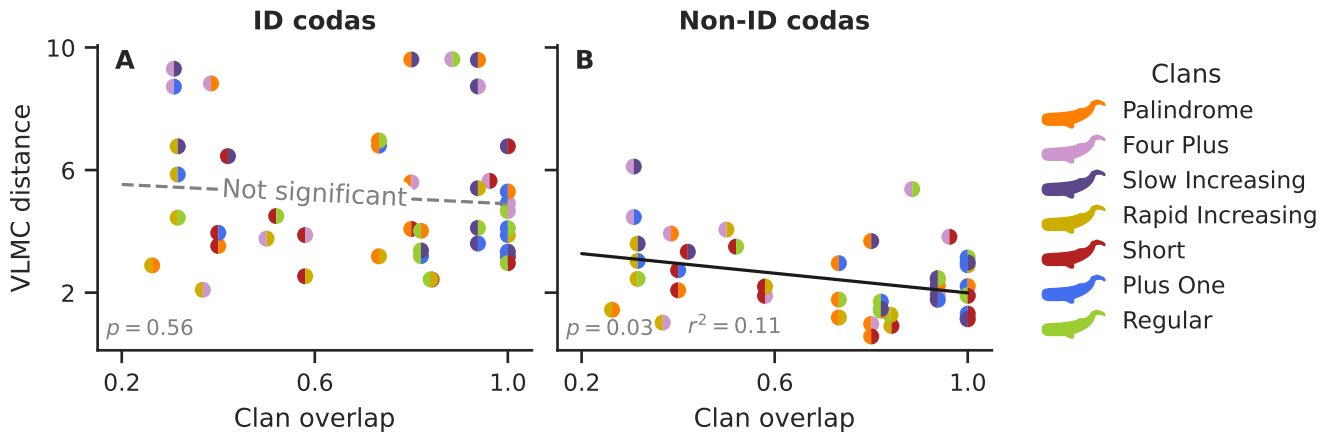


FIG. 4. **Clan overlap influences non-ID coda vocal styles** Comparing the similarities of different VLMC models fit for each Pacific Ocean clan for both ID and non-ID coda repertoires. The y-axis represents the measured distance between the subcoda trees, and the x-axis shows the geographical clan overlap (as calculated in [10]). Each point represents a pairwise comparison between two clans. Note how the effect of overlap on ID coda vocal style similarity is minimal and non-significant while the opposite is true for non-ID codas: overlapping clans produce non-ID codas with a more similar vocal style. The VLMC distances are also typically much greater for ID codas than for non-ID codas.

consider the functional role of ID versus non-ID codas.

More precisely, different clans can share significant portions of their total range, overlapping across large swaths of ocean. Such sympatric clans exhibit a decreasing similarity of their ID coda usage repertoires with increasing clan overlap [10]. This means that the more two clans overlap in space, the more dissimilar their vocal repertoires are in terms of ID coda types and usage. This is consistent with the idea that ID codas are used as symbolic markers to delineate cultural boundaries between social groups [8, 10]. In contrast, non-ID coda usage repertoires do not show any relationship to clan overlap.

We find the exact *opposite* effect when considering vocal style. The similarity in vocal style for ID codas across clans does not depend on the level of clan overlap (Fig. 4a). In contrast, the similarity in vocal style for non-ID codas displays a clear and significant increase (i.e., decreasing subcoda tree-distance) as clan spatial overlap increases (Fig. 4b). In the *Supplementary Materials* (see Section 2.4.2), we show that the same results hold at the single coda type level, in addition to the whole clan level. These results imply that the coda assembly process of non-ID codas is more similar for groups that likely spend more time in the same space, akin to accents aligning in human populations that share the same territory [23, 24].

## DISCUSSION

We have presented a general method for modeling animal communication systems and their complexity based on VLMCs. In the context of sperm whales, this new method allows the extraction of *subcoda trees*, which suc-

cinctly describe the internal temporal structure of codas. Previous work on the structure of sperm whale communication has largely focused on supra-level coda analyses: for example, by classifying codas into types, quantifying how often different types are used, and distinguishing between individual whales, social units, or clans based on those counts [16, 25]. Here, we adopted a more fine-scale approach by investigating potential structure *within* codas. To do so, we used VLMCs to model the transition probability of observing a specific ICI given the previous ones. A VLMC encodes all those probabilities for ICI sequences that are informative and discards sequences that are not. As such, the VLMC is a statistically validated representation of the internal memory structure of codas at the level of sequences of clicks. What it describes is not the usage frequency of codas, but rather how these codas are internally structured: a vocal style.

Using such representations, we propose a novel concept of *vocal identity* for sperm whales composed of *vocal repertoire* (what they say) and *vocal style* (how they say it), the latter being captured by our framework. We find that: (i) vocal styles vary between social units and clans, and can be used to distinguish them; (ii) the similarity of clan vocal styles for non-ID codas increases with increasing spatial overlap, while no change occurs for ID codas; and (iii) social learning across symbolic cultural boundaries most parsimoniously explains the observed trends.

### Vocal style recovers hierarchical social structure

Using the Dominica dataset, sperm whales had previously been divided into two vocal clans, based on their vocal repertoires and observed social interactions [19].

In our study, comparing the vocal styles of those same whales led to the same assignment of social units to two vocal clans. Similarly, for the Pacific dataset, clustering based on vocal styles yielded clans that were in good agreement with those previously defined based on vocal repertoires [10] (*Supplementary Materials* for an extended comparison). The difference between the two partitions was mainly due to the Short clan, which was more spread out in subcoda tree space than the other clans, causing overlap with other clans that showed less variability. This variability could be linked to the fact that Short clan whales typically make codas with very few (e.g., three or four) clicks, leading to subcoda trees with very few nodes. In [10] the authors observe a similar lack of uniformity in coda usage repertoires of the Short clan.

### Identity and non-identity codas show different trends

For ID codas, we show here that the similarity between clan vocal styles is not affected by spatial overlap, while it has been recently shown that the similarity between clan vocal repertoires decreases with overlap [10]. In contrast, for non-ID codas, we show here that the similarity between vocal styles increases with spatial overlap between two clans, while no change was observed for vocal repertoires [10]. Our study and that of Hersh et al. [10] combine to provide further support for ID codas being used by sperm whales as identity signals. While clan designations may be reconstructed based on vocal style alone, the contrasting results between these studies suggest that selection is acting to produce unambiguous, recognizable identity signals in the ID codas. Although we are able to discriminate among clans using vocal style, the shared nature of such vocal styles across clans and variation with spatial overlap demonstrated here suggests that these are likely vocal cues and not identity signals like the ID codas, which appear to be the product of selection favoring the ease of identification by conspecifics [26, 27]. However, ID codas only account for 35% of the total vocalizations; the remaining 65% of codas have traditionally been lumped into a catch-all category (i.e., non-ID codas) and their function remains enigmatic (these numbers are an average over the Pacific clans, and go up to 93% for non-ID codas when counting coda types instead of codas emitted, see SM 1.1 for details). Accordingly, vocal repertoire and vocal style capture different and complementary information on sperm whale communication.

### Evidence for social learning across cultural boundaries

There are several potential mechanisms driving the similarity in non-ID coda vocal styles across spatially overlapped clans: environmental variation, genetics, and/or social learning.

Local adaptation to specific ecological conditions can lead to geographic variation in acoustic signals [28]. If environmental pressures alone were responsible for the trends we observe in sperm whales, this would imply that (i) more spatially overlapped clans experience more similar environments, (ii) non-ID coda vocal style is impacted by or dependent on environmental parameters, and (iii) ID coda vocal style is not impacted by/dependent on environmental parameters. Although the first point is somewhat intuitive, to date there is no evidence that coda production systematically varies with environment. In fact, clans are recognizable across ocean basins, making local adaptation an unlikely driver of the observed trend in non-ID coda vocal style.

If genetic relatedness were responsible, this would imply that (i) non-ID coda vocal styles are genetically inherited, (ii) ID coda vocal styles are not genetically inherited, and (iii) more spatially overlapped clans are more genetically related. Existing research supports that coda repertoires are socially learned, not genetically inherited [20]. Furthermore, Rendell et al. [29] found little evidence to support genetics as an explanation of differences in vocal dialects among clans in the Pacific Ocean, and we find no reason why this would be different for vocal style.

The most parsimonious explanation for the observed similarity of non-ID coda vocal styles of clans with increasing spatial overlap is social learning across clan boundaries. Indeed, while sperm whales belonging to different clans have rarely been observed physically interacting at sea, this does not preclude the possibility that they are within acoustic range of each other [30] and that cross-cultural social learning opportunities arise. This explanation is compatible with (and bolsters) past work suggesting that ID and non-ID codas function differently in sperm whale communication, and further suggests that they experience different evolutionary pressures [20]. Whether social learning has facilitated stochastic (i.e., cultural drift) or deterministic (i.e., cultural selection) processes is more difficult to determine, and it is unclear whether the observed non-ID coda vocal style alignment has been neutral or adaptive [28, 31]. Importantly, these findings indicate that vocal learning in sperm whales is not limited to vertical transmission from mothers to offspring, but that horizontal and/or oblique social learning (from outside the natal social unit) are occurring as well. Furthermore, if non-ID coda vocal style is maintained over time, it would suggest that adult sperm whales learn as well.

Vocal identity in sperm whales is thus consistent with both cultural selection on identity codas to maintain discrete signals for vocal recognition in sympatry, and social learning between clans leading to a vocal style more similar to that of other whales with which they are in acoustic contact more frequently. This highlights a more complex system of transmission in which clan identity is maintained through selection, while gradual change over time may occur within and across clans for vocalizations

which do not function in social recognition and thus may create vocal styles.

### Future directions

Our results can be expanded in multiple ways in future work. The first, and the simplest conceptually, would be to conduct the present analysis on a larger dataset. More codas would improve the quality of the statistical analyses and ensure that all codas are represented in realistic proportions for each clan. Moreover, longitudinal datasets might provide direct evidence to discriminate between the social learning hypothesis and competing ones (e.g. drift in vocal style). Similarly, confirmations could emerge from large scale genetic datasets addressing the issues of phylogenetic relatedness (or lack thereof) in clans that are closer in vocal style distance. Such datasets do not exist at present, but efforts towards automated and semi-automated collection techniques are underway (e.g. Project CETI [32]). Second, from a methodological perspective, we could add spectral information (in terms of acoustic frequencies) to the temporal information currently used. Although sperm whale acoustic communication seems mostly based on rhythm, spectral features of individual clicks may convey additional information. This possibility could be incorporated into our method by labeling the dICIs according to the frequency content of the associated click (or by extending the available "alphabet" for the VLMC). Third, it would be interesting to investigate in more detail the function of non-ID codas. Indeed, even though ID codas were only recently formally named for the first time, they have been the primary focus of sperm whale coda research for decades. As previously mentioned, non-ID codas are a catch-all category for anything that is not an ID coda, but that does not mean that all non-ID codas function in the same way. To start to unveil their function, we need to consider the context (behavioral, environmental, etc.) in which different non-ID codas are produced [33]. The pattern we documented may or may not apply to all non-ID codas, but it is at least strong enough that we detect the relationship with clan spatial overlap when collectively considering all non-ID codas.

## METHODS

### Acoustic data

In social situations, sperm whales acoustically communicate through short bursts of *clicks* with recognizable patterns based on rhythm and tempo referred to as *codas*. Codas are generally represented as sequences of ICIs, equivalent to a time series of click onsets.

We analyzed two datasets in the present study. The Dominica dataset contains 8719 annotated codas recorded in the Atlantic Ocean off the island of Dominica

between 2005 and 2019. The codas come from 12 social units grouped into two vocal clans (EC1 and EC2). The Pacific dataset was collected between 1978 and 2017 at 23 locations in the Pacific Ocean (the recording methods are available in the supplementary materials of [10]). The codas were divided into repertoires according to their recording day and each repertoire was assigned a single vocal clan inferred in [10]. When considering a clan-level analysis (Fig. 3) all repertoires were used to compute the subcoda trees (23555 codas). However, when analysing at a repertoire level (Fig. 4), we discarded repertoires with less than 200 codas with statistical inference in mind, resulting in a final count of 57 repertoires (17046 codas) for the Pacific.

### Representation of sperm whale communication as discrete inter-click intervals

As a preliminary step, we discretized the (continuous) ICI values into bins of width  $\delta t$  seconds. In other words, we represented the continuum of ICI values by a finite set of discrete ICIs (dICIs) based on the duration of the ICI. The bin width  $\delta t$  controls the *temporal resolution* of the representation: a higher value of  $\delta t$  implies a coarser representation with fewer dICIs. We also imposed an upper bound  $t_{\max}$ : any ICI value greater than that was truncated to  $t_{\max}$ . This ensured that the set of dICIs was finite. Note that although ICIs have units of time (seconds), dICIs are unitless (they represent time intervals). The resulting representation of ICIs as dICIs is a discrete random variable defined as

$$X_{\delta t, t_{\max}} = \left\lfloor \frac{\min(\text{ICI}, t_{\max})}{\delta t} \right\rfloor, \quad (1)$$

which takes values in the finite set  $\mathcal{X} = \{0, 1, \dots, \lfloor \frac{t_{\max}}{\delta t} \rfloor\}$ . We represented the sequences of ICIs by sequences of dICIs from that finite set. Note that any ICI value above  $t_{\max}$  is mapped to the dICI  $\lfloor \frac{t_{\max}}{\delta t} \rfloor$  and therefore represents the end of a coda. We set  $t_{\max} = 1$  (longer than any ICI) and  $\delta t = 0.05$  throughout the analysis (see *Supplementary Materials* section 3.3.2 for justification of this choice and section 3.4.3 for an analysis on the influence of this parameter).

### Variable length Markov chains

We then modeled these dICI sequences using variable length Markov chains (VLMCs). VLMCs provide the large memory advantage of higher-order Markov chains when needed, without the drawback of having too many unnecessary parameters in the model.

Fitting a VLMC is the process of deciding how much memory is necessary to model specific sequences. The criterion for making this decision is the following: longer sequences are discarded if their distribution of transition probabilities is similar to that of shorter subsequences.

This process is often called *context tree estimation* and consists of two steps.

The first step is to consider  $\mathcal{W}_D$  the set of all sequences of maximum length  $D$  (which we set to 10) and to assign the following probability distribution  $q_w$  to each sequence:

$$q_w = P(X|w), \quad (2)$$

that is, the probability of observing a state  $x \in \mathcal{X}$  given the sequence  $w$ .

The second step is to prune the sequences that do not add information. Take two sequences  $u, w \in \mathcal{W}_D$ , one being the suffix of the other  $w = \sigma u$ . The information gained  $H_w$  by considering the longer sequence can be measured with a weighted Kullback-Leibler (KL) divergence  $D_{KL}$  [34]. The longer memory sequence  $w$  is kept only if the information gain is greater than some threshold  $K$  [35, 36]

$$\Delta H_w = N(w)D_{KL}(q_w||q_u) > K \quad (3)$$

where  $N(w)$  denotes the length of sequence  $w$ . Sequences that satisfy this condition are called *contexts* and sequences that do not are discarded. A VLMC can be defined as the set of these contexts  $w$  and their associated probability distribution  $q_w$  (see *Supplementary Materials* section 3.1 for details).

A VLMC can be visualized as a tree by representing each context  $w$  by a node and setting the root node as the context of length zero. Contexts that are subsequences of each other are then part of the same branches, which end with the longest contexts.

### Quantitative Comparison of VLMCs

If two VLMC models  $T_1$  and  $T_2$  are built over the same finite set of dICIs  $\mathcal{X}$ , there exists a map  $\phi_1 : \mathcal{W}_D \rightarrow T_1$  that maps any sequence of elements of  $\mathcal{X}$  into the longest sequence present in  $T_1$ , and similarly for  $T_2$ . This map also induces a map between the probability distributions of  $T_1$  and  $T_2$ . Given two distributions over the same set  $\mathcal{X}$ , we can measure how different they are with the *KL* divergence. Therefore, it is possible to define a dissimilarity between  $T_1$  and  $T_2$  by considering the average *KL* divergence over all sequences of  $T_1$  and their map  $\phi_1(T_2) \subseteq T_1$

$$d_{KL}(T_1, T_2) = \frac{1}{|T_1|} \sum_{w \in T_1} D_{KL}(q_w || p_{\phi_1(w)}) \quad (4)$$

Refer to the *Supplementary Materials* section 3.4 for a more detailed explanation.

This results in a dissimilarity measure that captures not just the difference in emission distribution but also the structural differences of the associated context trees. When comparing the distribution of distances in Fig. 2A and Fig. 3A we performed a *Kolmogorov-Smirnov* test to test if the distances between

social units/repertoires of the same clan and distances between social units/repertoires of different clans had come from the same distribution. For every pair, we can reject the hypothesis of the distances coming from the same distribution with 95% confidence.

### Hierarchical Clustering of VLMCs

The dendrograms in Fig. 2B and Fig. 3B were obtained by hierarchical clustering using average linkage on the set of subcodon trees (VLMCs). Since the distance is not symmetric, for agglomerative clustering we considered the symmetric distance:

$$d_{KL}(T_1, T_2) = \max \{d_{KL}(T_1, T_2), d_{KL}(T_2, T_1)\}. \quad (5)$$

### Measuring clan overlap

We used the clan spatial overlap values from [10]. Briefly, given two clans A and B, and the repertoires associated to them, the amount of geographical overlap of A in B was measured as the fraction of repertoires belonging to clan A that were recorded within 1000 kilometers of at least one repertoire of clan B.

### Statistical Testing

On Fig. 2 and Fig. 3 we compare the distributions of distances between subcodon trees of of repertoires/social units of the same clan (*within*) and of different clans (*between*). The purpose is to assess whether these distributions originate from the same underlying population. We employ both the *Kolmogorov-Smirnov* test and the *T*-test. The observed *p*-values were well below 0.01 for all clans. This allows us to confidently reject the hypothesis that there is no difference between the vocal style between different clans. For more information check the *Supplementary Materials* in section 3.4.2.

To assess the existence of a relationship between clan overlap and vocal style similarity, we applied an ordinary least squares linear regression model (OLS). We show the resulting *p* values of the OLS statistical test at the bottom left of each plot of Fig. 4 along with the observed  $r^2$  value.

### ACKNOWLEDGMENTS

This study was funded by Project CETI via grants from Dalio Philanthropies and Ocean X; Sea Grape Foundation; Rosamund Zander/Hansjorg Wyss, Chris Anderson/Jacqueline Novogratz through The Audacious Project: a collaborative funding initiative housed at TED. TAH was supported by Independent Max Planck Research Group Leader funding to Andrea Ravnani of

the Max Planck Institute for Psycholinguistics. The Dominica coda dataset originates from The Dominica Sperm Whale Project which was supported by a FNU fellowship for the Danish Council for Independent Research supplemented by a Sapere Aude Research Talent Award, a Carlsberg Foundation expedition grant, a grant from Focused on Nature, two Explorer Grants from the National Geographic Society (all to SG), and supplementary grants from the Arizona Center for Nature Conservation, Quarters For Conservation, the Dansk Akustisks Selskab, Oticon Foundation, and the Dansk Tennis Fond. Further funding was provided by Discovery and Equipment grants from the Natural Sciences and Engineering Research Council of Canada to Hal Whitehead (Dalhousie University) and a FNU large frame grant and a

Villum Foundation Grant to Peter Madsen (Aarhus University). The publicly accessible Pacific Ocean sperm whale coda dataset we used in this study emanates from the Global Coda Dialect Project, a consortium of scientists conducting sperm whale acoustics research worldwide. Members of the consortium who contributed to the Pacific Ocean dataset include: Luke Rendell, Maurício Cantor, Lindy Weilgart, Masao Amano, Steve M. Dawson, Elisabeth Slooten, Christopher M. Johnson, Iain Kerr, Roger Payne, Andy Rogan, Ricardo Antunes, Olive Andrews, Elizabeth L. Ferguson, Cory Ann Hom-Weaver, Thomas F. Norris, Yvonne M. Barkley, Karlina P. Merkens, Erin M. Oleson, Thomas Doniol-Valcroze, James F. Pilkington, Jonathan Gordon, Manuel Fernandes, Marta Guerra, Leigh Hickmott and Hal Whitehead.

- 
- [1] L. Rendell and H. Whitehead, Culture in whales and dolphins, *Behav. Brain Sci.* **24**, 309–324 (2001).
- [2] A. Whiten, F. J. Ayala, M. W. Feldman, and K. N. Laland, The extension of biology through culture, *Proc. Natl. Acad. Sci.* **114**, 7775 (2017).
- [3] H. Whitehead and L. Rendell, The cultural lives of whales and dolphins, in *The Cultural Lives of Whales and Dolphins* (University of Chicago Press, 2014).
- [4] P. Slater, The cultural transmission of bird song, *Trends Ecol. Evol.* **1**, 94 (1986).
- [5] L. V. Luncz, R. M. Wittig, and C. Boesch, Primate archaeology reveals cultural transmission in wild chimpanzees (pan troglodytes verus), *Philos. Trans. R. Soc. B* **370**, 20140348 (2015).
- [6] S. Alem, C. J. Perry, X. Zhu, O. J. Loukola, T. Ingraham, E. Søvik, and L. Chittka, Associative mechanisms allow for social learning and cultural transmission of string pulling in an insect, *PLoS Biol.* **14**, e1002564 (2016).
- [7] F. Barth, Introduction, in *Ethnic Groups and Boundaries* (Little Brown, 1969).
- [8] R. McElreath, R. Boyd, and P. Richerson, Shared norms and the evolution of ethnic markers, *Curr. Anthropol.* **44**, 122 (2003).
- [9] R. Boyd and P. J. Richerson, The evolution of ethnic markers, *Cult Anthropol* **2**, 65 (1987).
- [10] T. A. Hersh, S. Gero, L. Rendell, M. Cantor, L. Weilgart, M. Amano, S. M. Dawson, E. Slooten, C. M. Johnson, I. Kerr, R. Payne, A. Rogan, R. Antunes, O. Andrews, E. L. Ferguson, C. A. Hom-Weaver, T. F. Norris, Y. M. Barkley, K. P. Merkens, E. M. Oleson, T. Doniol-Valcroze, J. F. Pilkington, J. Gordon, M. Fernandes, M. Guerra, L. Hickmott, and H. Whitehead, Evidence from sperm whale clans of symbolic marking in non-human cultures, *Proc. Natl. Acad. Sci.* **119**, e2201692119 (2022).
- [11] M. Cantor, S. Gero, H. Whitehead, and L. Rendell, Sperm whale, the largest toothed creature on earth, in *Ethology and behavioral ecology odontocetes* (Springer, 2019) pp. 261–280.
- [12] W. A. Watkins and W. E. Schevill, Sperm whale codas, *J. Acoust. Soc. Am.* **62**, 1485 (1977).
- [13] T. A. Hersh, S. Gero, L. Rendell, and H. Whitehead, Using identity calls to detect structure in acoustic datasets, *Methods Ecol. Evol.* **12**, 1668 (2021).
- [14] L. Weilgart and H. Whitehead, Coda communication by sperm whales (*Physeter macrocephalus*) off the Galápagos Islands, *Can. J. Zool.* **71**, 744 (1993).
- [15] T. Schulz, H. Whitehead, S. Gero, and L. Rendell, Individual vocal production in a sperm whale (*physeter macrocephalus*) social unit, *Mar. Mammal Sci.* **27**, 149 (2010).
- [16] S. Gero, H. Whitehead, and L. Rendell, Individual, unit and vocal clan level identity cues in sperm whale codas, *R. Soc. Open Sci.* **3**, 150372 (2016).
- [17] L. Rendell and H. Whitehead, Spatial and temporal variation in sperm whale coda vocalizations: stable usage and local dialects, *Anim. Behav.* **70**, 191 (2005).
- [18] L. E. Rendell and H. Whitehead, Vocal clans in sperm whales (*Physeter macrocephalus*), *Proc. Royal Soc. B* **270**, 225 (2003).
- [19] S. Gero, A. Böttcher, H. Whitehead, and P. T. Madsen, Socially segregated, sympatric sperm whale clans in the Atlantic Ocean, *R. Soc. Open Sci.* **3**, 160061 (2016).
- [20] M. Cantor, L. G. Shoemaker, R. B. Cabral, C. O. Flores, M. Varga, and H. Whitehead, Multilevel animal societies can emerge from cultural transmission, *Nat. Commun.* **6**, 8091 (2015).
- [21] P. C. Bermant, M. M. Bronstein, R. J. Wood, S. Gero, and D. F. Gruber, Deep Machine Learning Techniques for the Detection and Classification of Sperm Whale Bioacoustics, *Sci. Rep.* **9**, 12588 (2019).
- [22] F. Vachon, T. Hersh, L. Rendell, S. Gero, and H. Whitehead, Ocean nomads or island specialists? culturally driven habitat partitioning contrasts in scale between geographically isolated sperm whale populations, *R. Soc. Open Sci.* **9**, 211737 (2022).
- [23] E. Cohen, The evolution of tag-based cooperation in humans: The case for accent, *Curr. Anthropol.* **53**, 588 (2012).
- [24] J. Henrich and M. Muthukrishna, The origins and psychology of human cooperation, *Annu. Rev. Psychol.* **72**, 207 (2021).
- [25] C. Oliveira, M. Wahlberg, M. A. Silva, M. Johnson, R. Antunes, D. M. Wisniewska, A. Fais, J. Gonçalves, and P. T. Madsen, Sperm whale codas may encode individuality as well as clan identity, *J. Acoust. Soc. Am.*

- 139**, 2860 (2016).
- [26] T. Peake, P. Mcgregor, K. Smith, G. Tyler, G. Gilbert, and R. G. RE, Individuality in corncrake *crex crex* vocalizations, *Ibis* **140**, 120–127 (1998).
  - [27] T. Bergman and M. Sheehan, Social knowledge and signals in primates, *Am. J. Primatol.* **75**, 683–694 (2013).
  - [28] K. Sun, L. Luo, R. T. Kimball, X. Wei, L. Jin, T. Jiang, G. Li, and J. Feng, Geographic variation in the acoustic traits of greater horseshoe bats: testing the importance of drift and ecological selection in evolutionary processes, *PLoS One* **8**, e70368 (2013).
  - [29] L. Rendell, S. L. Mesnick, M. L. Dalebout, J. Burtenshaw, and H. Whitehead, Can genetic differences explain vocal dialect variation in sperm whales, *physeter macrocephalus?*, *Behav. Genet.* **42**, 332 (2012).
  - [30] P. Madsen, M. Wahlberg, and B. Møhl, Male sperm whale (*physeter macrocephalus*) acoustics in a high-latitude habitat: implications for echolocation and communication, *Behav. Ecol. Sociobiol.* **53**, 31 (2002).
  - [31] V. B. Deecke, J. K. Ford, and P. Spong, Dialect change in resident killer whales: implications for vocal learning and cultural transmission, *Anim. Behav.* **60**, 629 (2000).
  - [32] J. Andreas, G. Beguš, M. M. Bronstein, R. Diamant, D. Delaney, S. Gero, S. Goldwasser, D. F. Gruber, S. de Haas, P. Malkin, *et al.*, Towards understanding the communication in sperm whales, *iScience* **25**, 104393 (2022).
  - [33] A. Frantzis and P. Alexiadou, Male sperm whale (*physeter macrocephalus*) coda production and coda-type usage depend on the presence of conspecifics and the behavioural context, *Can. J. Zool.* **86**, 62 (2008).
  - [34] S. Kullback and R. A. Leibler, On information and sufficiency, *Ann. Math. Stat.* **22**, 79 (1951).
  - [35] M. Mächler and P. Bühlmann, Variable length markov chains: methodology, computing, and software, *J. Comput. Graph. Stat.* **13**, 435 (2004).
  - [36] A. Galves, C. Galves, J. E. Garcia, N. L. Garcia, and F. Leonardi, Context tree selection and linguistic rhythm retrieval from written texts, *Ann. Appl. Stat.* **6**, 186 (2012).
  - [37] P. Cénac, B. Chauvin, F. Paccaut, and N. Pouyanne, *Variable length markov chains and dynamical sources* (2010).
  - [38] J. Gustafsson, P. Norberg, J. R. Qvick-Wester, and A. Schliep, Fast parallel construction of variable-length markov chains, *BMC Bioinform.* **22**, 1 (2021).
  - [39] J. C. Chang, Predictive bayesian selection of multistep markov chains, applied to the detection of the hot hand and other statistical dependencies in free throws, *R. Soc. Open Sci.* **6**, 182174 (2019).
  - [40] H. Akaike, A new look at the statistical model identification, *IEEE Trans. Automat.* **19**, 716 (1974).
  - [41] H. Tong, Determination of the order of a markov chain by akaike’s information criterion, *J. Appl. Probab.* **12**, 488 (1975).

# Supplementary Material: Social learning across symbolic cultural barriers in non-human cultures

## I. DATA AND PREPROCESSING

Sperm whales communicate vocally via *clicks*: short bursts of sound emitted in sequence. These clicks are combined into recognizable patterns called *codas*. Clicking sperm whales were recorded with a hydrophone, and clicks were detected in the resulting audio files by human experts. The data that we used consists of time sequences of inter-click intervals (ICIs), i.e. the times between two consecutive detected clicks—this is equivalent to having a time series of click onsets.

We used two datasets: the Dominica and Pacific datasets. The Dominica dataset contains 8719 annotated codas recorded in the Atlantic Ocean near Dominica. The codas come from 12 social units grouped into two vocal clans (EC1 and EC2). The Pacific dataset consists of around 23555 codas recorded between 1978 and 2017 in 23 Pacific Ocean locations. The codas were divided into repertoires according to their recording day and each repertoire was assigned a single vocal clan inferred in [10]. When considering a clan-level analysis all repertoires were used to compute the VLMC models. However when analysing at a repertoire level, we discarded repertoires with less than 200 codas with statistical inference in mind, resulting in a final count of 57 repertoires (17046 codas) for the Pacific.

To model the ICI sequences in the datasets, we represented the ICIs by a finite set of symbols (or states), in three main steps (Fig. S1). First, we denoted  $X$  a continuous random variable that represents an ICI:

$$X = \text{ICI}. \quad (\text{S1})$$

Second, we imposed an upper bound  $t_{\max}$  on the values taken by  $X$ . This was to make sure that we are modeling with a finite number of states. Specially, in situations here the maximum number of states have to be known. We set this value to 1 second to be sure that it is longer than any ICI.

$$X_{t_{\max}} = \min(\text{ICI}, t_{\max}). \quad (\text{S2})$$

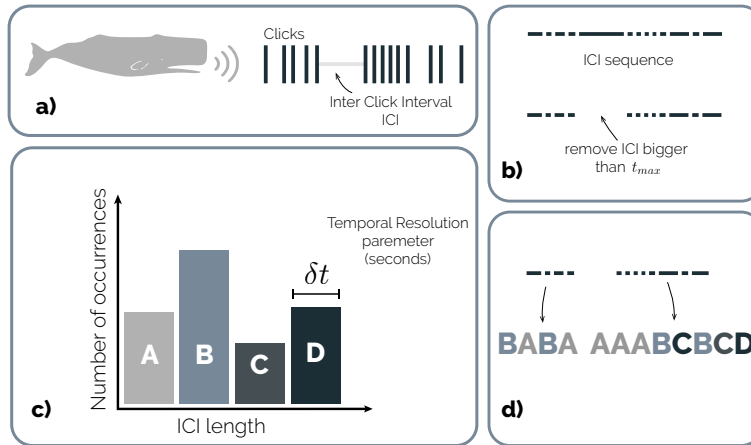


FIG. S1. **Representing sperm whale communication as a sequence of symbols.** **a** The temporal patterns of click onsets are equivalently encoded as sequences of inter-click intervals (ICIs). **b** We discard ICI values larger than a threshold  $t_{\max}$  seconds, and **(c)** discretize the others into a finite set of bins of width  $\delta t$  seconds. Each bin is then assigned a symbol (here a letter of the Latin alphabet), so that each symbol represents an ICI in a given range. **d** We then represent sperm whale communication as a sequence of these symbols.

Thirdly and finally, we discretized the values of the ICIs into a set of bins, akin to a histogram. We denote  $\delta t$  the width of these bins in seconds and call it the *temporal resolution* of the representation. Formally, we define

$$X_{\delta t, t_{\max}} = \left\lfloor \frac{\min(\text{ICI}, t_{\max})}{\delta t} \right\rfloor. \quad (\text{S3})$$

By construction, this defines a discrete random variable that takes values in the finite set  $\mathcal{X} = \{0, 1, \dots, \lfloor \frac{t_{\max}}{\delta t} \rfloor\}$ . Note that each element of this set represents a range of ICI values of length  $\delta t$  seconds. Any ICI value above  $t_{\max}$  is

mapped to the symbol  $\lfloor \frac{t_{\max}}{\delta t} \rfloor$ . It thus represents the end of a coda. We set the upper bound to  $t_{\max} = 1$  seconds and  $\delta t = 0.05$  (see Section III C for details about the choice of values).

We then modeled sperm whale communication sequences  $(X_i)_{i \in \mathbb{N}}$ . In addition, for clarity, we will denote the elements of  $\mathcal{X}$  by letters of the Latin alphabet  $A, B$ , and so on. In terms of terminology, we will also refer to  $\mathcal{X}$  as an alphabet, and to its elements as symbols or states, interchangeably.

### A. ID and non-ID codas

Some coda types are considered ID for some clans but non-ID for others. The Pacific dataset [10] has annotations specifying this label (ID or non-ID) for each coda and each clan. For each clan, we counted the total number of codas that are ID and the total number of codas that are not (see Table S1).

TABLE S1. Count of Codas

Clan Name	Total	ID	Non-ID	Percentage of ID
Four Plus (FP)	2590	587	2003	22.66%
Palindrome (PALI)	2124	1249	875	58.8%
Plus One (PO)	2083	1252	831	60.11%
Regular (REG)	8289	3545	4744	42.77%
Rapid Increasing (RI)	1776	425	1351	23.93%
Short (SH)	5428	562	4866	10.35%
Slow Increasing (SI)	1265	541	724	42.77%
Total	23555	8161	15394	34.65%

We also provide similar statistics for the count of different coda types (see Table S2).

TABLE S2. Count of Coda Types

Clan Name	Total	ID	Non-ID	Percentage of ID
Four Plus (FP)	72	2	70	2.78%
Palindrome (PALI)	64	9	55	14.06%
Plus One (PO)	54	6	48	11.11%
Regular (REG)	74	9	65	12.16%
Rapid Increasing (RI)	79	2	77	2.53%
Short (SH)	85	1	84	1.18%
Slow Increasing (SI)	59	3	56	5.08%
Total	487	32	455	6.57%

## II. THE ROLE OF MEMORY

A coda is a series of clicks emitted in fast succession. They have traditionally been identified by practitioners as building blocks for sperm whale communication. Whether or not codas themselves are composed by series of smaller collections of clicks is however an open question. We asked: are the codas the smallest such blocks, or is there structure at a scale shorter than codas—but longer than the individual clicks that constitute them? In order to answer this, we modeled sperm whale communication as higher-order Markov chains, that is, Markov chains with a memory  $h$  larger than or equal to one (but of fixed length)—see Section II for details. In other words, we assume that the probability of observing an ICI within given range—here referred to as symbol or state—depends on the  $h$  previous states. For a given  $h$ , we fit this Markov model to the data by estimating the transition probabilities from sequence of  $h$  state to any other state.

The results are summarized in Fig. S2, for a range of memory values  $h$ , and for two temporal resolutions for the binning of the ICIs. We note that there is a bifurcation between two different behaviors around  $h \approx 3$ : transition probabilities go from very low (approximately random transitions) to very large (almost deterministic transitions). Indeed, for  $h < 3$ , these probabilities are very low [Fig. S2(a)] and all similar [Fig. S2(b)]. All possible next states are equally likely, but not very likely: this indicates underfitting. On the contrary, for  $h > 3$ , the transition probabilities are all close to one and all similar. Moreover, only a few of them are non-zero [Fig. S2(c)]. Given a sequence longer than three, only one next state can be observed: this indicates overfitting. Finally, for  $h \approx 3$ , transition probabilities are heterogeneous: their average is between 0 and 1, their variance exhibits a peak, and more than one state can

potentially be observed next. Moreover, the Akaike Information Criterion (AIC) displays a minimum around that value of the memory, which indicates that it provides a good trade-off between variance of the data explained and the number of parameters needed for the model.

This transition around  $h \approx 3$  suggests that there is structure at that level of memory, which is shorter than most coda types. This motivates our search for structure within codas. However, fixed-memory Markov Chains do not allow for different configurations to have different levels of memory, which leads to variable length Markov Chains (described in the next section).

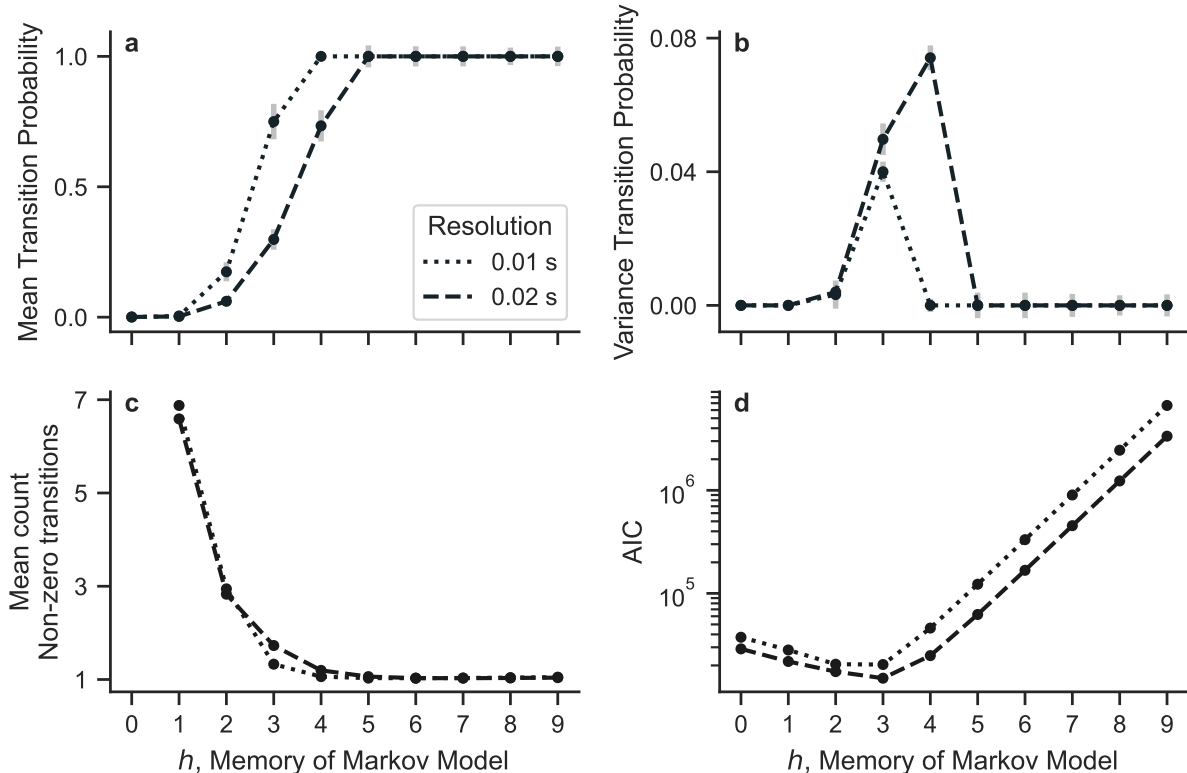


FIG. S2. **Fixed length Markov model bifurcates as a function of memory length  $h$ .** We show (a) the mean, and (b) the variance of the transition probabilities as a function of  $h$ . We also show (c) the number of non-zero transition probabilities per state, and (d) the AIC. The dashed and dotted lines represent two different temporal resolutions (i.e., bin size used during Preprocessing). There is a bifurcation around  $h \approx 3$  that suggests sub-coda structure.

### III. VARIABLE LENGTH MARKOV CHAINS

Some states can be predicted with more or less memory of past states than others. This observation is the base motivation for introducing variable length Markov Chains (VLMCs) which go beyond the fixed-memory limit of traditional Markov chains. Take for example a state  $X_2$  that has the same probability of occurring knowing the last two states ( $x_0 x_1 \in \mathcal{X}^2$ ) or only the last state ( $x_1 \in \mathcal{X}^1$ ):

$$P(X_2|x_0, x_1) = P(X_2|x_1). \quad (\text{S4})$$

In this case, a shorter memory ( $h = 1$ ) is sufficient and we do not need a longer one ( $h_2$ ).

In practice, VLMCs bypass the necessity of having  $(n-1)n^h$  parameters by allowing states to have unequal lengths (memory). Smaller lengths are preferred whenever the additional memory does not significantly change the distribution of transitions to the next possible states.

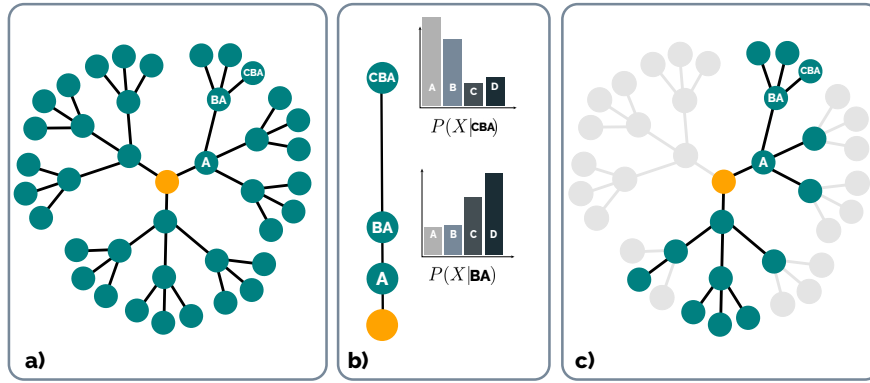


FIG. S3. Steps for fitting a VLMC from a sequence. Step 1 (a): Construction of the full (or saturated) suffix tree up to maximum depth  $D$ . Step 2 (b): Assigning a probability measure to every element of the tree. Step 3 (c) Pruning of nodes that carry the same information content as parents according to Eq. (S10). In this example, context  $CBA$  is relevant because it changes the distribution of transition probabilities with respect to its parent  $BA$  and therefore it is not pruned.

### A. Building a VLMC

For a Markov model of fixed order  $h$ , the set of possible states  $\mathcal{X}^h$  is composed of all possible sequences of length  $h$ . For a VLMC, however, states can be sequences of arbitrary length. The set of possible states is thus a subset of the set of all sequences that can be built from the alphabet  $\mathcal{X}$ , including the empty sequence  $\mathcal{X}^0 = \emptyset$ . Let  $\mathcal{W}$  denote this set.

$$\mathcal{W} = \bigcup_i^{\infty} \mathcal{X}^i \quad (\text{S5})$$

In this project, because codas are typically constructed from a small number of clicks, we only consider *finite* length sequences (see [37] for non-finite VLMCs). In practice, we choose a *maximum* memory allowed  $D$ , which we set to  $D = 10$ , much larger than the typical coda length.

$$\mathcal{W}_D = \bigcup_i^{D=10} \mathcal{X}^i \quad (\text{S6})$$

Fitting a VLMC is the process of finding some subset  $\mathcal{L} \subseteq \mathcal{W}_D$  where the elements satisfy the condition: shorter states are preferred if their distribution of transition probabilities is similar to their longer length equivalents. This is generally called context tree estimation in the literature [38].

**Probabilising the tree** We start with  $\mathcal{W}_D$  for some  $D$  which we take to be equal to 10. To each element of  $w \in \mathcal{W}_D$  we assign a probability distribution  $q_w$  over the set  $\mathcal{X}$  as the probability of observing a state  $x \in \mathcal{X}$  given a previous sequence  $w$ .

$$q_w = P(X|w) \quad (\text{S7})$$

Where  $P$  denotes the likelihood estimation computed as

$$q_w(X = x) = P(X = x|w) = \frac{N(wx)}{\sum_{c \in \mathcal{X}} N(wc)} \quad (\text{S8})$$

where  $N(w)$  the number of occurrences of the sequence  $w$ .

**Pruning the tree** Given two sequences  $u, w \in \mathcal{W}_D$ , we say that  $u$  is a suffix of  $w$  if  $w = \sigma u$  for some other sequence  $\sigma$  of length  $\geq 1$ . If  $\sigma \in \mathcal{X}$  we say that  $u$  is a parent of  $w$ . That is,  $u$  is a parent of  $w$  if  $u$  is a suffix of  $w$  and  $w$  is longer by only one letter.

In an intuitive way,  $u$  is a parent of  $w$  if  $w$  “looks into the past” one step further than  $u$ . At the core of the VLMC is measuring the information gain in using the longer memory  $u$  instead of its shorter memory parent  $w$ . If this information gain is not sufficient, then we discard the longer memory  $u$ . We measure the information gain in using the longer memory  $w$  instead of  $u$  with a weighted Kullback-Leibler (KL) divergence  $D_{KL}$  [34]:

$$\begin{aligned}\Delta H_w &= N(w)D_{KL}(q_w||q_u) \\ &= N(w)\sum_{x\in\mathcal{X}}P(x|w)\log\frac{P(x|w)}{P(x|u)}\end{aligned}\tag{S9}$$

The longer memory sequence  $w$  is kept if and only if the information gain is greater than some threshold  $K$  [35, 36]. Refer to Section III C for a discussion on the value of  $K$ . The set of all sequences that respect the above threshold are called *contexts*, and denoted by  $T$ :

$$T = \{w \in \mathcal{W}_D | \Delta H_w > K\}\tag{S10}$$

A VLMC is the the Markov model with the set of states:

$$\mathcal{L} = \{wx \mid t \in T, x \in \mathcal{X}\}\tag{S11}$$

and with transition probabilities defined by  $q_w$  for  $w \in T$ .

## B. Model Selection

When modeling a process  $(X_i)_{i\in\mathbb{N}}$  with a Markov model, the memory length  $h$  controls the trade-off between complexity and error. Higher memory values tend to result in models that generalize poorly. On the other hand, lower values of  $h$  fail to capture the patterns, resulting in a uniformly random model.

To choose an appropriate value of  $h$ , it is common to employ some statistic that measures the trade-off between precision in prediction and the number of parameters. A model with high predictability and a low number of parameters is favored. There is a wide range of metrics [39] and one of the most widely used is the AIC [40, 41]:

$$\text{AIC} = 2k - 2 \log \hat{P}((X_i)_{i\in\mathbb{N}}|\mathcal{M}_h).\tag{S12}$$

$\hat{P}((X_i)_{i\in\mathbb{N}}|\mathcal{M}_h)$  is the maximum likelihood of the sequence  $(X_i)_{i\in\mathbb{N}}$  given the Markov model  $\mathcal{M}_h$  with memory length  $h$  and  $k$  parameters (transition probabilities). The best model is indicated by the lowest AIC.

## C. Parameter sensitivity

### *Information gain threshold $K$*

The threshold value  $K$  represents the minimum information gain necessary to increment the memory of a given context by one. This value ultimately influences the depth and shape of the VLMC model. Low thresholds result in deep trees with many parameters and are prone to overfitting, whereas small threshold values cause trees to not expand past low values of memory and potentially fail to capture statistical dependencies (Fig. S4).

The best value of  $K$  should be the one that outputs the optimal VLMC model (i.e., the one that minimizes the AIC).

$$\arg \min_{T \subseteq \mathcal{W}_D} \text{AIC}(T)\tag{S13}$$

However, this search is done over the entire set of possible context trees. The problem of estimating the optimal context tree is an ongoing research area although many good methods have been proposed [36].

For some threshold  $K$ . The above dissimilarity is an expression of differences of deviances and as such follows an asymptotic  $\frac{1}{2}\chi^2$  distribution [35] with  $|\mathcal{X}| - 1$  degrees of freedom. As such we can set the  $K$  thresholds to represent quantiles of a  $\chi^2$  distribution. We use the 0.95 quantile, meaning we keep the child whose additional memory exceeds the value:

$$K = \frac{1}{2}\chi_{|\mathcal{X}|-1,0.95}^2\tag{S14}$$

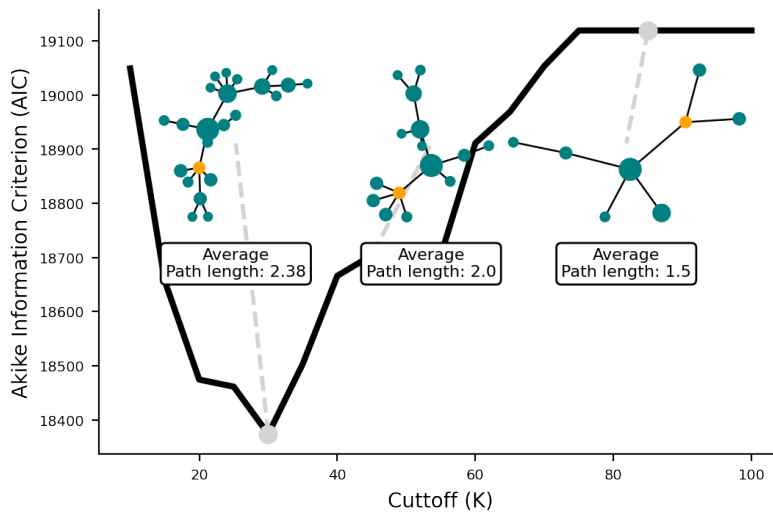


FIG. S4. **Selecting the optimal information cutoff  $K$ .** The AIC for different VLMC models with respect to the cutoff value ( $K$ ) used to build them. Above are some context trees associated with three different VLMCs. The trees decrease in size for the threshold increases since the information gain has to be greater for a context to be “accepted” in the tree. This effect is also visible in the average path length which can be seen as the average memory of the model.

#### Temporal resolution $\delta t$

The temporal resolution  $\delta t$  denotes the scale at which we discretize the continuous, absolute ICI values into bins. A small value might provide differentiation between clicks, but also burdens the VLMC models by increasing the number of parameters and states.

To select the most appropriate resolution parameter, one might be tempted to compare the AIC obtained from different VLMC models extracted from data at different resolutions. However, that is not possible since models fit on different data are not really comparable. Imagine the extreme case with a time resolution so large that all clicks are mapped to the same discrete symbol: any model fit on this data would achieve an optimal AIC value.

In our case, we compare the AIC obtained from the VLMC model with the AIC obtained from a fixed length Markov model of order 0 fitted to the same aggregated data. The intuition behind this approach is that the zero length Markov model represents how “easy” it is to predict the data. The best resolution would be the one where the difference between the AIC of our fit VLMC is the biggest when compared to the  $0^{\text{th}}$  order Markov model (Fig. S5).

#### D. Quantitative comparison of VLMCs

The KL divergence is one of the most used methods for measuring statistical dissimilarity between two distributions, mostly due to its connections to information-theory. Being a generative model, a VLMC is not a single probability distribution, but a set of distributions  $q_w$  one for each context  $w \in T$ .

Given two VLMC models  $T_1$  and  $T_2$  over the same alphabet  $\mathcal{X}$ . Let  $p$  and  $q$  be their associated sets of transitions distributions, respectively. We define the divergence  $d_{KL}(T_1, T_2)$  between them as the average KL divergence between the set of associated transition distributions.

However, there may not be a one-to-one map between  $q_w$  and  $p_w$ . In fact, more often than not  $T_1$  and  $T_2$  have a different number of contexts. As such, for every  $w \in T_1$  we associate  $u \in T_2$  where  $u$  is the longest suffix of  $w$  that belongs to  $T_2$ . This results in a dissimilarity measure that captures not just the difference in emission distribution but also the structural differences of the associated context trees:

**Divergence** Given two VLMCs  $(T_1, (q_w)_{w \in T_1})$  and  $(T_2, (p_w)_{w \in T_2})$  built over the finite alphabet  $\mathcal{X}$  we define the distance:

$$\begin{aligned}
 d_{KL}(T_1, T_2) &= \frac{1}{|T_1|} \sum_{w \in T_1} D_{KL} \left( q_w \parallel p_{\overleftarrow{\text{pref}(w)}} \right) \\
 &= \frac{1}{|T_1|} \sum_{w \in T_1} \sum_{x \in \mathcal{X}} q_w \log \frac{q_w}{p_{\overleftarrow{\text{pref}(w)}}}
 \end{aligned} \tag{S15}$$

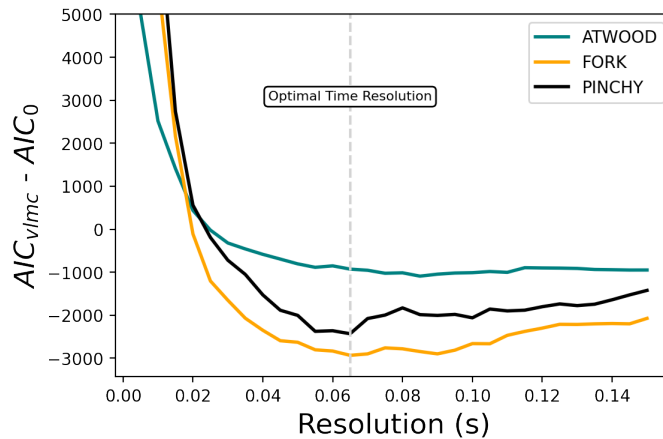


FIG. S5. **Selecting the optimal temporal resolution.** The temporal resolution parameter  $\delta t$  for the preprocessing steps is chosen by subtracting the AIC of the 0th order memory Markov model from the AIC of a VLMC model, which encodes how well the model predict versus how easy it is to predict the data. We use this setup because the AIC alone is not sufficient, because the actual fitted dataset changes with the resolution parameter, and thus models with different  $\delta t$  are not directly comparable. The minimum value is the best resolution parameter although any value between 0.01 and 0.1 seems acceptable. We show this for three individual sperm whales (colors) from the Dominica dataset.

Where  $\overleftarrow{\text{pref}}(w)$  denotes the longest suffix of  $w \in T_1$  that belongs to  $T_2$ .

$$\overleftarrow{\text{pref}} : T_1 \rightarrow T_2 \quad (\text{S16})$$

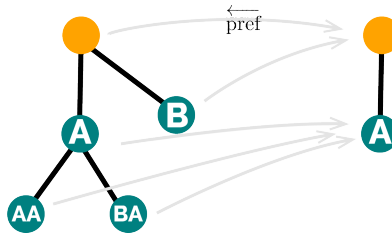


FIG. S6. **Measuring dissimilarity between two VLMC models.** The two trees represent two VLMCs models built over the same alphabet  $\mathcal{X}$ . We measure their dissimilarity or distance with the KL divergence.

#### Statistical testing on distribution of the distances

We fit a VLMC model on repertoires/social units from different clans on both the Pacific and Dominica dataset. For each clan we compute the distances between all VLMC models belonging to that clan (*within*) and between the models of the clan to the ones belonging to other clans (*between*) (Fig. S7). On each pair (*within/between*) we tested the distributions to check if they both came from the same populations. We employed both the *Kolmogorov-Smirnov* test and the *T-Test*. We also measured the effect size using *Cohen's* method. The resulting statistics for both datasets can be found in the tables below.

#### Non-ID results by coda type

In this section we repeat the approach on comparing the geographical clan overlap with the VLMC distance on non-ID codas. In contrast to the main text, we segment each set of codas by coda type and note the slope, the p-value of the Pearson correlation and the p-value according to a Spearman correlation, Table S4. Just as the main text, when segmenting by coda type we observe that the vast majority of correlations is negative, i.e., geographically

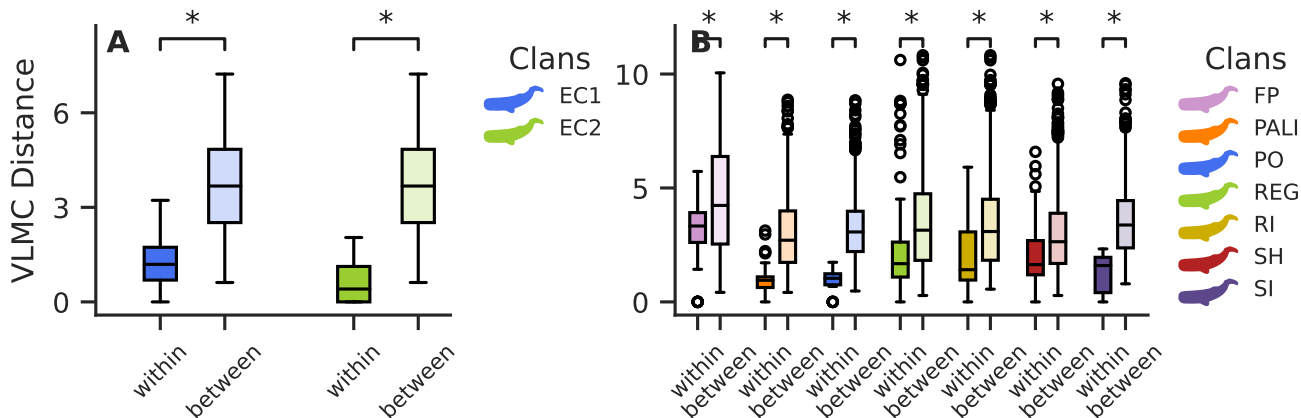


FIG. S7. **Comparison of the distribution of distances between VLMC models, with statistical significance.** Each color represents a clan of a given dataset: Pacific **A**) and Dominica **B**). The *within* distribution represents the distance between VLMC models fit on elements of the same clan. The *between* represent the distance between VLMC models of different clans.

TABLE S3. **Distance distribution statistics.** Table with the  $p$ -values and the effect size corresponding to the comparison of the *within/between* distance distributions of repertoires of codas from the Dominica clans (top) and the Pacific clans (bottom), under the Kolmogorov-Smirnov (K-S test) and the T-Test.

Clan	K-S test	T-test	Effect Size
EC1	$1.5 \times 10^{-16}$	$1 \times 10^{-24}$	-2.4
EC2	0.0019	0.0006	-1.9
Four Plus	$1.7 \times 10^{-7}$	$6.2 \times 10^{-6}$	-0.67
Palindrome	$6.7 \times 10^{-17}$	$6.7 \times 10^{-13}$	-1.3
Plus One	$6.9 \times 10^{-21}$	$2.4 \times 10^{-14}$	-1.6
Regular	$4.2 \times 10^{-27}$	$7.2 \times 10^{-28}$	-0.76
Rapid Increasing	0.00016	0.0005	-0.72
Short	$6.5 \times 10^{-14}$	$9.9 \times 10^{-18}$	-0.67
Slow Increasing	$1.6 \times 10^{-9}$	$1.6 \times 10^{-7}$	-1.4

overlapped clans have a more similar communication. However, although most correlations are negative, only a small portion is significant. It is important to take into consideration that the amount of data used to fit each VLMC model is considerably reduced given the extra segmentation. Furthermore, coda types that were uttered exclusively by only two clans were also omitted as it is always possible to draw a line between two points, and thus a linear analysis makes little sense.

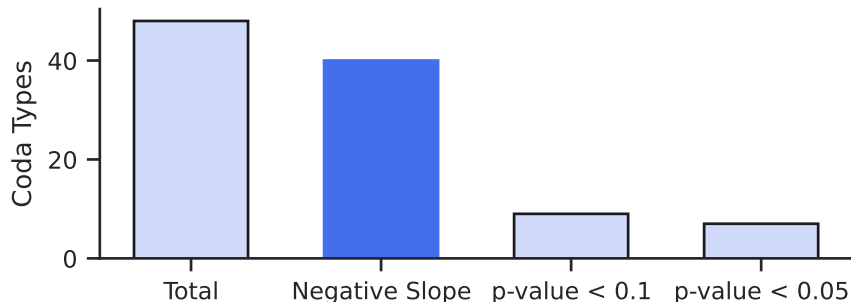


FIG. S8. **VLMC distance and geographical overlap relation by coda type.** each bar represents a number of unique coda types. Note that almost all coda types have a negative correlation with geographical overlap, although only a small portion is significant. The  $p$ -values shown are with respect to the Pearson correlation, Table S4

TABLE S4. **Geographical overlap and subcoda distance by coda type.** Results of comparing the geographical overlap and VLMC distance segmented by coda types. Negative correlations are highlighted as well as p-values that are below 0.05. "Number of Clans" represents how many clans where compared.

Coda Type	Slope	Pearson-P	Spearman-P	Number of Clans
33	<b>-0.353</b>	0.864	0.787	3
34	<b>-0.944</b>	0.257	0.050	4
35	<b>-6.022</b>	<b>0.031</b>	<b>0.032</b>	5
42	<b>-4.098</b>	<b>0.004</b>	<b>0.010</b>	7
43	<b>-0.615</b>	0.596	0.573	4
45	<b>-1.327</b>	0.266	0.207	5
47	<b>-5.808</b>	0.628	0.700	3
48	9.818	0.258	0.257	3
49	10.481	0.371	0.538	3
51	<b>-0.939</b>	0.634	0.695	6
52	<b>-1.663</b>	<b>0.002</b>	<b>0.021</b>	7
53	<b>-3.341</b>	<b>0.017</b>	0.075	6
55	0.522	0.909	0.752	4
57	<b>-3.480</b>	0.410	0.511	4
58	<b>-0.896</b>	0.755	0.623	3
61	<b>-1.512</b>	<b>0.074</b>	<b>0.006</b>	7
64	<b>-1.651</b>	0.061	0.276	5
66	<b>-2.482</b>	0.138	0.062	7
67	<b>-2.782</b>	0.172	0.269	6
71	<b>-1.994</b>	0.870	0.518	3
72	<b>-0.041</b>	0.979	0.856	7
73	<b>-1.334</b>	0.337	0.329	3
76	<b>-0.981</b>	0.681	0.829	7
77	<b>-4.093</b>	0.141	0.093	5
79	<b>-1.116</b>	0.268	0.142	5
82	<b>-0.847</b>	0.265	0.266	3
83	0.908	0.578	0.284	6
85	<b>-1.473</b>	<b>0.044</b>	<b>0.032</b>	4
86	<b>-0.089</b>	0.845	0.600	3
88	2.831	<b>0.000</b>	<b>0.000</b>	7
91	<b>-2.662</b>	0.254	0.387	6
93	0.613	0.597	0.618	6
310	<b>-4.118</b>	0.320	0.193	4
311	<b>-1.554</b>	0.170	<b>0.016</b>	6
312	<b>-1.275</b>	0.325	0.069	6
313	<b>-3.087</b>	0.475	0.186	4
315	<b>-1.189</b>	0.593	0.700	3
411	0.489	0.711	0.795	4
412	<b>-2.092</b>	0.578	0.700	3
414	<b>-2.269</b>	<b>0.012</b>	<b>0.006</b>	7
511	<b>-3.246</b>	<b>0.038</b>	0.059	7
513	<b>-1.806</b>	0.174	0.107	7
514	<b>-0.449</b>	0.869	1.000	4
610	<b>-1.794</b>	0.145	0.123	7
612	5.633	0.486	0.618	3
613	<b>-0.426</b>	0.907	0.397	3
1011	<b>-1.081</b>	0.539	0.660	5
1012	<b>-0.966</b>	0.696	0.342	4

*Stability under different resolutions*

We also show that our results about the effect of sympatry on non-ID coda vocal styles hold for different values of the time resolution. That is, that the parameter preprocessing steps and the method parameters have little to no effect on the fundamental results of our approach. In Fig. S9 we repeat the analysis of the main text. We compare the geographical overlap with the distance between the VLMC of the pacific clans on both non-ID and ID codas.

We observe that regardless of the time resolution used in the method (for discretizing the continuous ICIs into

discrete ICIs), our results hold. That is, there is never a significant correlation between overlap and ID codas and that there is always a negative correlation between clan overlap and non-ID codas.

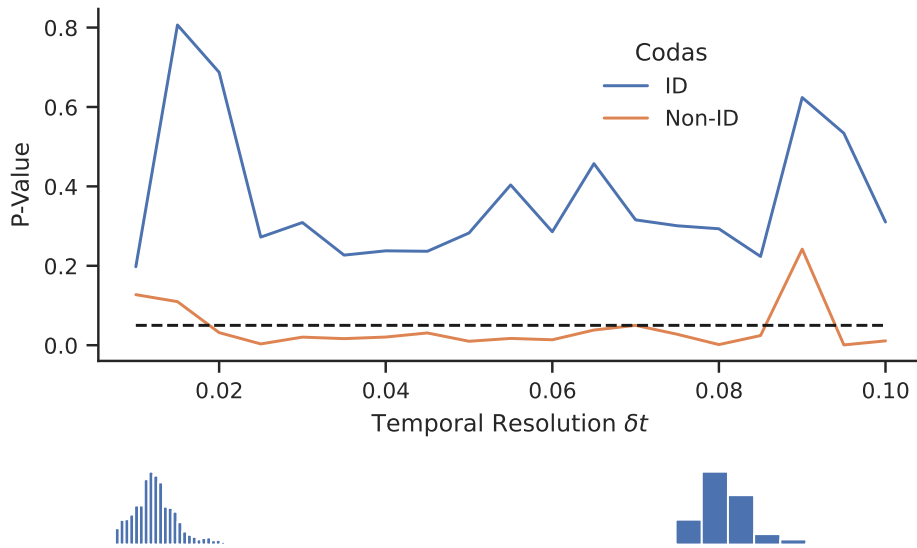


FIG. S9. **Results are significant for different resolutions.** The dotted line represents the 0.05 confidence value. When varying the time resolution used for fitting the VLMCs we observe that our main results persist: ID codas are not related with geographical overlap while non-ID codas always are. The bottom row shows two illustrations of the bin sizes (and subsequently the number of different states) resulting from the preprocessing using 0.01 and 0.1 seconds time resolution respectively.

#### Comparing Dendrograms

Using the distance between the VLMC trees it is possible to create a hierarchical plot of the repertoires. One can find it beneficial to compare our resulting hierarchical plot with the clan labels from [10] where the authors group the whales by coda type usage and divide the Pacific clans into the aforementioned 7 clans. However, comparing a dendrogram with a realized set of labels is not trivial. On the other hand, an effective comparison of two sets of labels can be achieved using the *Adjusted Rand Score*, or other entropy based metrics. The Adjusted Rand Score has a value of 0.0 for random labeling (independent of number of clusters) and 1.0 for clusters that match perfectly. The lowest possible score is  $-0.5$  for exceptionally disparate clusterings.

To obtain two sets of labels we progressively cut the dendrogram obtained by the VLMC and compared the set of labels with the clan labels from [10]. At each cut we calculate the adjusted rand score (results in Fig. S10). We observed a maximum value of 0.5. This reiterates not only the concordance with the pre-existing vocal usage clans but also emphasizes that vocal style is capturing new information at a different, lower, scale.

## IV. CLASSIFICATION OF SYNTHETIC CODAS

The fixed-length Markov chains described above lack flexibility: a model with large memory  $h$  generalizes better but requires estimating an ever-increasing number of parameters. For this reason, we then used VLMCs, which combine the best of both worlds by determining the optimal memory needed for each transition individually. Essentially, we keep a transition probability with a longer memory  $P(X_i|x_jx_k)$  only if it changes the distribution sufficiently compared to a short memory one  $P(X_i|x_j)$ .

A VLMC can be naturally visualized as a tree, where the concept of order arises from the fact that shorter memory contexts are subsequences of longer ones. In Fig. S11A and B, we show examples of two VLMCs computed from data from a single sperm whale each. The visual structure of these trees can be related to the actual information-theoretic structure of these sperm whales' communication. Indeed, the root node is represented in orange, and nodes that are depth  $h$  in the tree (that is  $h$  edges away from the root node) represent context (or sequences) of memory  $h$ . To verify that the structure we observe actually contains information, we need to compare it to the structure of a null model.

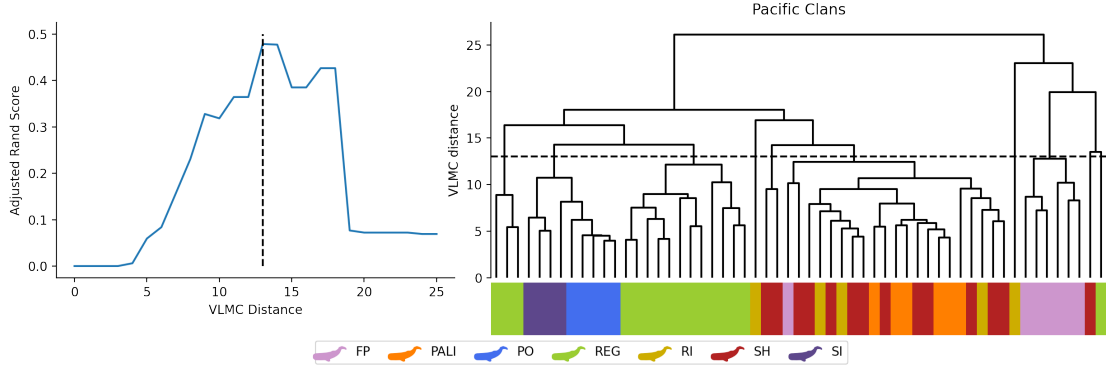


FIG. S10. **Adjusted Rand Score for VLMC clustering dendrogram** Comparison of the dendrogram obtained from the VLMC distance between the trees with the vocal clan labels. The values of the Adjusted Rand Score go from -0.5 to 1.

To do this, we took the same ICI time series used to build the tree from Fig. S11A, and randomly shuffled its ICIs. This way, all temporal information is lost. This results in a tree that has no structure, as shown in Fig. S11C. The VLMC-indicated structure can thus be interpreted as coming from the sperm whale communication.

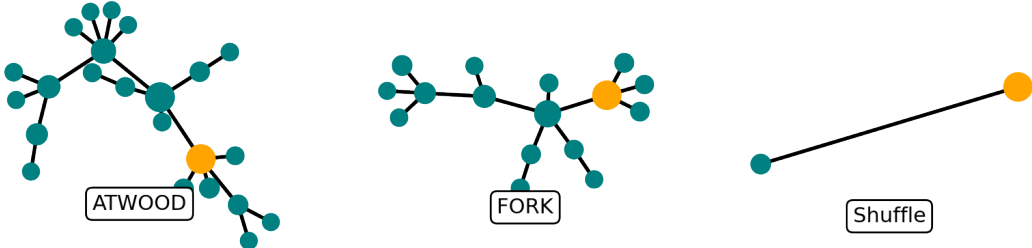


FIG. S11. **VLMCs capture structure of sperm whale communication.** We show context trees associated with the variable length models built for two individual sperm whales: (a) *ATWOOD*, and (b) *FORK*. For comparison, we show (c) the corresponding tree after randomly shuffling ICIs from the same timeseries data used to build (a). Note how the shuffled version does not exhibit any structure. The orange node represents the root node, and the size of each node represents the number of occurrences of the associated context.

Having confirmed that our VLMCs capture some communication structure, we ask: What and how much structure does it capture? To answer this, we took advantage of two facts. First, the VLMCs can be used to generate new codas by generating sequences of states that correspond to ICIs. Indeed, like for any Markov model, we can start from the empty sequence, and start adding suffixes with probabilities defined by the model (see Methods). In other words, we can generate synthetic data. Second, in [21] the authors present an LSTM-based classifier capable of assigning a coda to a specific clan with over 90% accuracy. We trained it on the original ICI data used to build our trees, achieving similar accuracy as shown by the black curve in Fig. S12. To verify how much information our VLMCs capture, we used that trained classifier on the synthetic codas generated with our trees. Remarkably, it classified the generated data with between 70 and 80% accuracy, depending on the temporal resolution  $\delta t$  (blue in Fig. S12). The fairly small difference in accuracy between the real and synthetic data indicates that a large part of the communication structure captured by the classifier in the real data is also captured by our VLMC models.

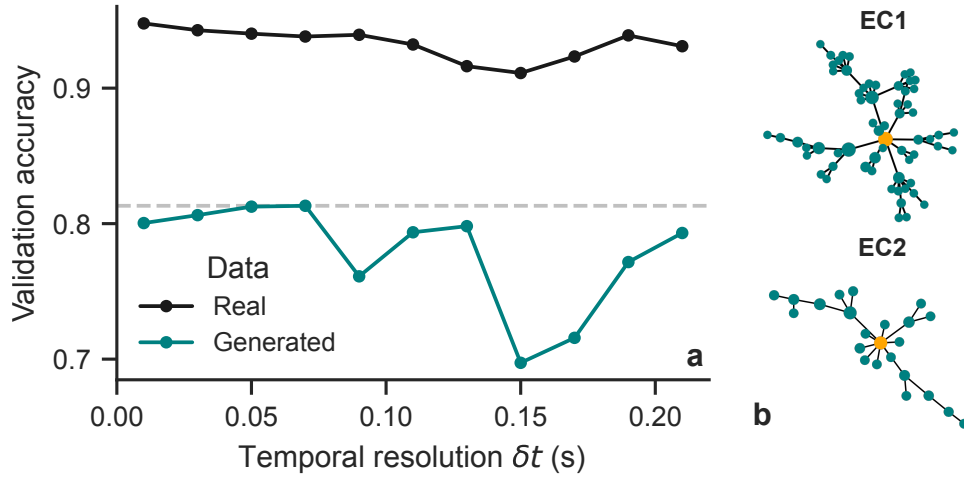


FIG. S12. **Deep learning classifier trained on real communication data generalises well to synthetic data generated by the VLMCs.** We show (a) the accuracy of the classifier on the real data (in black) and the synthetic data (in blue), as a function of the temporal resolution  $\delta t$ . The dashed grey curve highlights the maximum accuracy of on the generated data. The classifier's task was to identify to which of (b) two clans the data belonged to: EC1 or EC2.

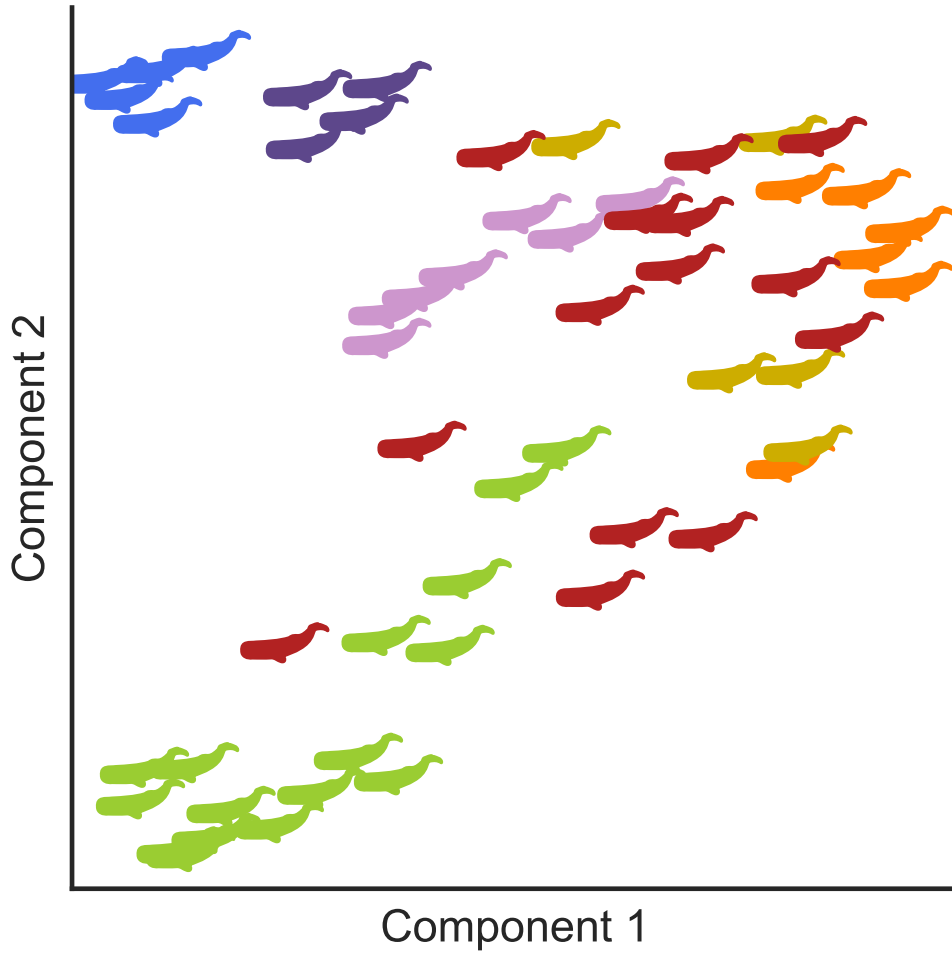


FIG. S13. **Vector Space embedding using UMAP** Embedding of all the Pacific Ocean clans according to their VLMC distance into two dimensions using UMAP.